Published in partnership with Nanjing Tech University



https://doi.org/10.1038/s41528-025-00408-5

Flexible perovskite light-emitting diodes: recent progress, applications and challenges

Check for updates

Ying Li^{1,6}, Tingyi Gao^{1,6}, Ziquan He^{2,6}, Chenxi Shen², Siqian Zhou², Mingze Li³, Daquan Zhang¹ ⊠, Qianpeng Zhang² ⊠, Yu Fu³ ⊠, Xiaoliang Mo², Zhaoyu Zhang¹, Wengang Bi¹ & Zhiyong Fan^{4,5} ⊠

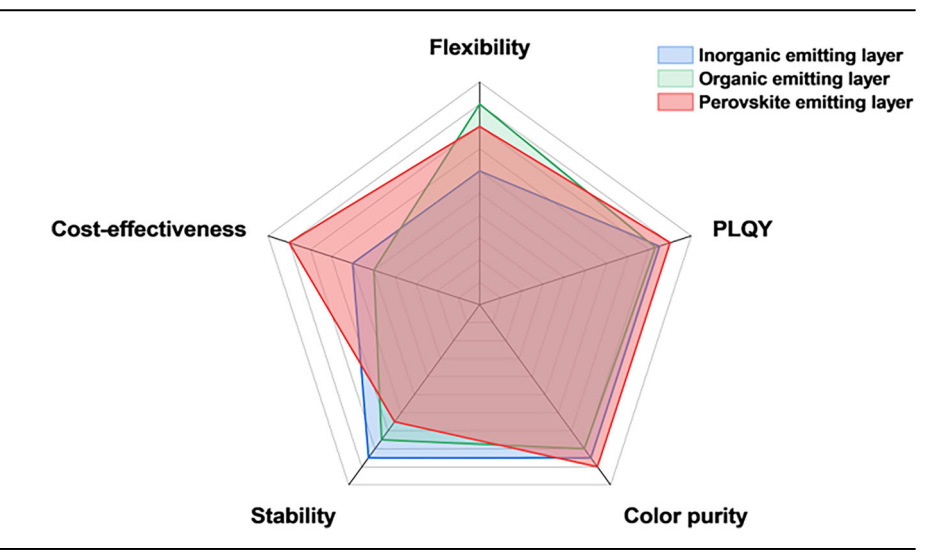
Significant progress has been made in perovskite light-emitting diodes (PeLEDs) over the past decade, with external quantum efficiencies (EQEs) exceeding 30% for green and red emissions, and 20% for blue emissions. However, the performance and device area of flexible PeLEDs remains constrained due to issues such as crack formation and short circuits that occur during device deformation. These challenges limit their applicability in flexible, stretchable, and wearable displays and lighting solutions. This review systematically summarizes recent advancements in flexible PeLEDs, focusing on various strategies to improve their flexibility and performance. We first discuss the use of flexible substrates and electrodes in these devices. Next, we examine the fabrication methods and the mechanical and optoelectronic properties of different perovskite materials used in flexible PeLEDs, including three-dimensional (3D) thin films, low-dimensional nanomaterials, and perovskite/polymer composites. Finally, we highlight the extensive applications of flexible PeLEDs in wearable optoelectronics and provide an outlook on the future development of high-performance flexible PeLEDs to facilitate their commercialization.

Flexible light-emitting diodes (FLEDs), recognized for their excellent mechanical properties and lightweight features, have garnered significant attention for a range of emerging optoelectronic technologies, such as unconventional lighting, flexible and foldable displays, consumer electronics, and healthcare monitoring¹⁻⁴. Currently, the predominant technology in FLEDs is based on organic LEDs (OLEDs), which utilize the deposition of organic light-emitting and charge transport materials onto flexible substrates⁵⁻⁷. Despite the advantages of OLEDs, including high EQE, color purity, and bending capabilities, the organic molecules or polymers used often require complex synthesis processes. Coupled with the high cost of these raw materials, this poses substantial barriers to device production, especially for large-sized flexible display panels^{8,9}. Moreover, the luminescent color of OLED materials depends on their chemical structure, and achieving color adjustments typically necessitates the synthesis of varied materials, which limits color tunability 10,11.

Recently, metal halide perovskite materials have emerged as promising candidates for high-performance LEDs, demonstrating substantial potential for next-generation displays and lighting solutions due to their excellent optical properties. Generally, metal halide perovskite can be expressed as the formula of ABX3, where "A" site is commonly occupied by monovalent cations such as methylamine (MA⁺), formamidine (FA⁺), and cesium (Cs⁺). "B" site is divalent metal cation like lead ion (Pb^{2+}) or tin ion (Sn^{2+}) , etc. And "X" represents halide anion including chloride ion (Cl⁻), iodide ion (I⁻), and bromide ion (Br⁻). The distinctive feature of perovskites is that ions at all sites can be substituted either completely or partially, allowing for bandgap tuning and thus influencing the emission wavelength. This compositional tunability endows perovskite materials with a broad color gamut. The unique bandgap structure of perovskites allows for high tolerance to shallow and intra-band defects, which is beneficial for realizing high photoluminescence quantum yield (PLQY). Additionally, compared to conventional commercialized OLEDs and quantum dots LEDs (QLEDs), PeLEDs

¹School of Science and Engineering, Shenzhen Key Laboratory of Semiconductor Laser, The Chinese University of Hong Kong, Shenzhen (CUHK-Shenzhen), Shenzhen, China. ²State Key Laboratory of Photovoltaic Science and Technology, Shanghai Frontiers Science Research Base of Intelligent Optoelectronics and Perception, Institute of Optoelectronics, Fudan University, Shanghai, China. ³School of Advanced Energy, Shenzhen Campus of Sun Yat-sen University, Shenzhen, China. ⁴Department of Electronic & Computer Engineering, State Key Laboratory of Advanced Displays and Optoelectronics Technologies, The Hong Kong University of Science and Technology, Clear Water Bay, Hong Kong SAR, China. ⁵Department of Chemical and Biological Engineering, The Hong Kong University of Science and Technology, Clear Water Bay, Hong Kong SAR, China. ⁵These authors contributed equally: Ying Li, Tingyi Gao, Ziquan He. ⊠e-mail: zhangdaguan@cuhk.edu.cn; zhang gp@fudan.edu.cn; fuvu37@mail.sysu.edu.cn; eezfan@ust.hk

Fig. 1 | Comparison of different emitting layers for FLEDs. The comparison of flexibility, PLQY, color purity, stability and cost-effectiveness among inorganic, organic and perovskite materials as emitting layers in FLEDs.



have higher color purity. The full width at half maximum of the electroluminescent emission peak of PeLEDs is typically ~20 nm, while the OLEDs and QLEDs are ~40 nm and 30 nm, respectively. This narrow emission bandwidth provides the potential for more vivid and accurate color reproduction in displays. Given these advantages, remarkable progress has been achieved on PeLEDs¹²⁻¹⁹. For instance, the EQE and Luminance of green PeLEDs have surpassed 32% and 1.1×10^6 cd m^{-2 20,21}, respectively, which is comparable to state-of-the-art OLEDs and QLEDs²²⁻²⁵. Additionally, unique low-temperature synthesis methods for perovskites, such as solution spin-coating and thermal evaporation, facilitate the fabrication of high-performance flexible PeLEDs²⁶⁻²⁸. By employing comprehensive optimization techniques, including active layer morphology manipulation, charge transport layer refinement, and light outcoupling efficiency enhancement, the EQE of flexible PeLEDs has significantly improved, achieving an impressive value of 24.5%²⁹. Unlike organic semiconductor materials, the lower cost of raw materials and simpler synthesis processes for flexible PeLEDs greatly reduce overall fabrication costs³⁰, essential for largescale FLED production and commercialization.

In addition to the color purity mentioned above, we also extracted relevant data from published studies to compare the flexibility³¹⁻⁴³, PLQY^{44–50}, materials cost⁵¹, and stability^{52–54} of flexible devices based on organic, inorganic, and perovskite light-emitting materials. Specifically, we analyzed Young's modulus values reported in the literature; organic materials typically exhibit lower Young's modulus (1-10 GPa), indicating higher flexibility, while inorganic materials have higher values (70-250 GPa), and perovskite materials fall in between 10-50 GPa. For PLQY, all three material types can achieve values exceeding 90%, demonstrating their potential for efficient light emission. Material costs were evaluated by comparing the prices of raw materials, with organic materials often being more expensive due to complex synthesis processes, while inorganic materials are relatively cheaper, and perovskite materials are the most cost-effective due to their simple synthesis processes and cheap raw materials, with costs significantly lower than those of organic and inorganic materials. Stability was assessed by comparing the operational lifetimes of LEDs, with inorganic LEDs showing excellent long-term stability, OLEDs have shown significant improvements through engineering techniques, and PeLEDs continue to make progress despite ongoing challenges. Figure 1 illustrates a comparison of these critical properties among three typical light-emitting materials. The overall performance of perovskite materials positions them as a promising candidate for next-generation FLED devices.

In this review, we systematically summarize the recent advancements in flexible PeLEDs while providing insights into this rapidly evolving and promising research field. We begin by discussing optimization strategies for flexible substrates and electrodes, which are critical for enhancing the

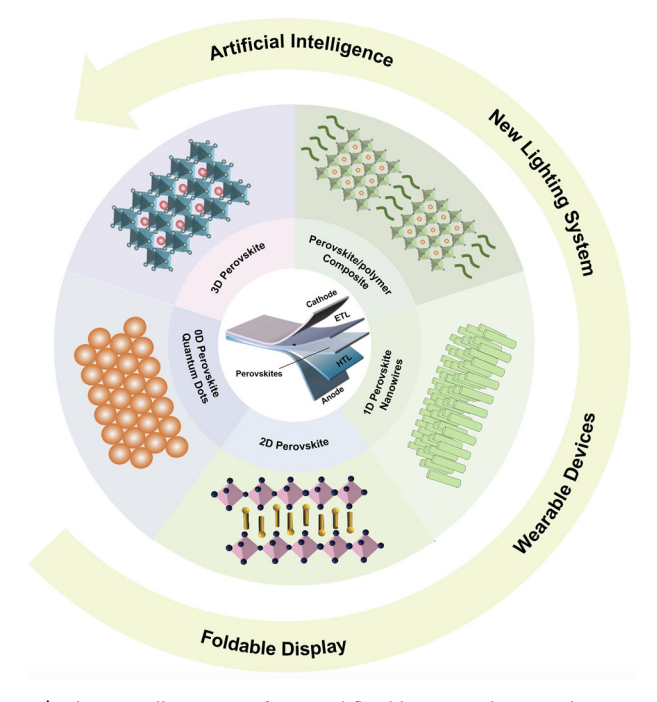


Fig. 2 | Schematic illustration of a typical flexible PeLED device with various perovskite materials as the light-emitting layer and their potential applications. The diversity of emitting layers in flexible PeLEDs provide versatile peroperties for the devices and flexible PeLEDs exhibited great potential in the future applications including artificial intellligence, new lighting system, wearable devices and foldable display equipments.

mechanical stability and performance of flexible PeLEDs. Subsequently, we classify perovskite morphologies and review the fabrication methods, mechanical and optoelectronic properties, and device performance of various flexible PeLEDs based on different types of perovskites. This includes 3D thin films, perovskite/polymer composites, two-dimensional (2D) and quasi-2D films, one-dimensional (1D) nanowires (NWs), and zero-dimensional (0D) quantum dots (QDs), as schematically depicted in Fig. 2. Each morphology presents unique advantages for flexible PeLED applications. We then discuss the progress in the application of flexible PeLEDs, emphasizing their potential in wearable and foldable display technologies. Finally, we outline the current challenges in fabricating high-performance flexible PeLEDs and explore potential avenues for their future development and commercialization.

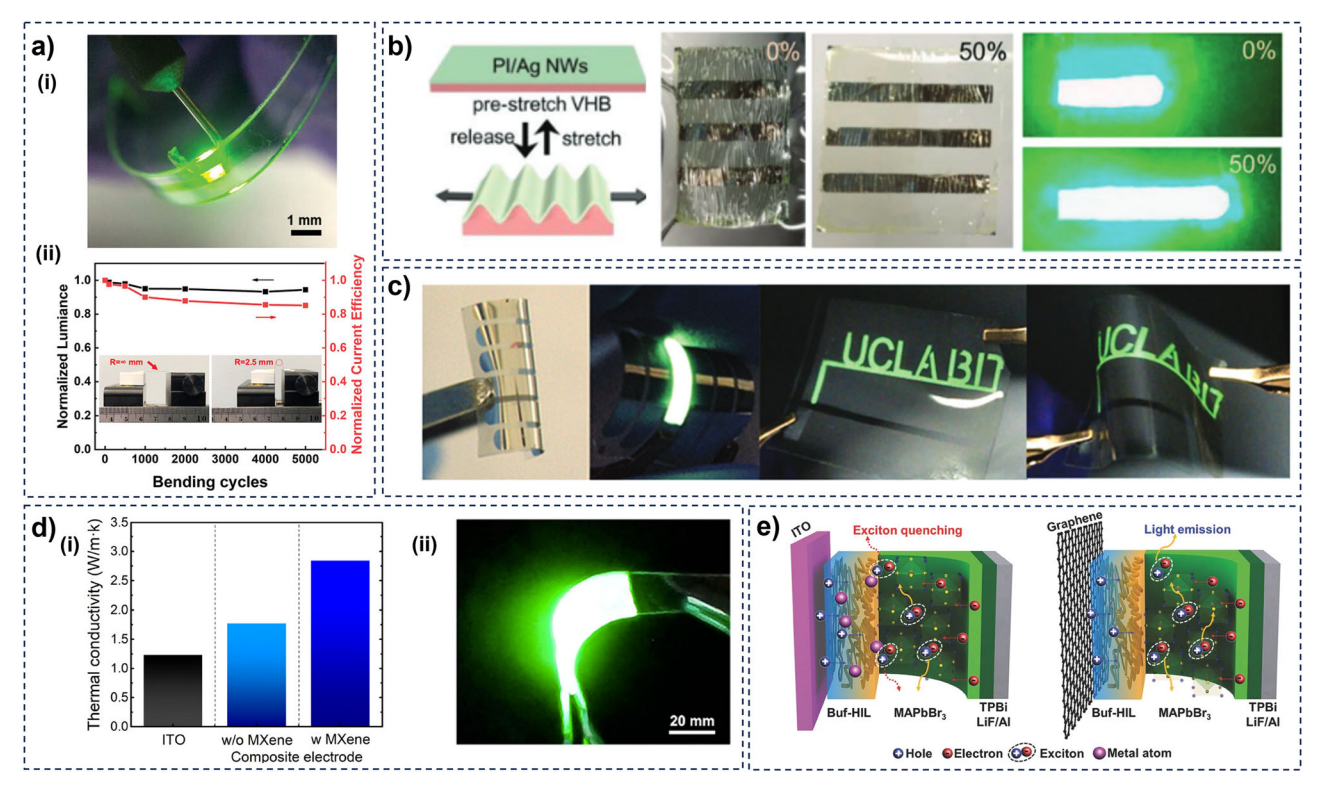


Fig. 3 | Flexible PeLEDs based on flexible substrates and electrodes, a A PeLED fabricated on a flexible PDMS substrate when being lit and bent to a curvature radius of 3.5 mm (i), and normalized luminance and current efficiency (CE) measured after 5000 bending cycles with a curvature radius of 2.5 mm (ii). Reproduced with permission from ref. 56. Copyright 2021, John Wiley and Sons. b Schematic illustration of the stretch/release process of PI/AgNWs composite electrode attached on a prestretched VHB, and digital photo of the stretchable PeLEDs under different strains with and without bias. Reproduced with permission from ref. 59. Copyright 2017,

John Wiley and Sons. $\bf c$ Digital photos of the flexible PeLEDs under different bending conditions. Reproduced with permission from ref. 60. Copyright 2017, Royal Society of Chemistry. $\bf d$ Thermal conductivities of different electrodes (i) and photograph of a large-area flexible PeLED with a size of 40 mm \times 20 mm operating at 5 V (ii). Reproduced with permission from ref. 61. Copyright 2022, American Chemical Society. $\bf e$ Schematic drawings of exciton quenching by In and Sn atoms in ITO-PeLEDs (i), and efficient light emission in Gr-PeLEDs (ii). Reproduced with permission from ref. 62. Copyright 2017, John Wiley and Sons.

Flexible PeLEDs based on flexible substrates and electrodes

Similar to traditional organic and inorganic materials, the fundamental approach to realizing flexible devices involves utilizing substrates and electrodes that boast high flexibility and transparency. Additionally, the performance of flexible PeLEDs is significantly influenced by the choice of substrates and electrodes. Therefore, optimizing the mechanical and electrical properties of substrates and electrodes has proven to be an effective strategy for enhancing the flexibility of flexible PeLEDs. For instance, Qin et al.⁵⁵ successfully deposited perovskite onto disposable label paper substrates, achieving an impressive EQE of 14.3%. Wang et al. deposited a perovskite emitting layer on an elastic polydimethylsiloxane (PDMS)/polyethylene terephthalate (PET) substrate, allowing the PeLEDs to exhibit exceptional durability; the luminance of the devices only dropped by 5.5% after 5000 bending cycles with a radius of curvature of 2.5 mm (Fig. 3a)⁵⁶.

The use of traditional electrodes in flexible devices often presents durability challenges, necessitating the integration of flexible conductive materials, such as graphene electrodes or silver nanowire (AgNW) composite films, to not only improve conductivity but also enhance the device's mechanical durability^{57,58}. Li et al. demonstrated the fabrication of flexible QD PeLEDs by adapting relatively rigid and non-stretchable perovskite stacked layers onto a wrinkled elastomer substrate⁵⁹. Specifically, they employed an ultrathin, smooth AgNWs/polyimide (PI) composite electrode to mechanically couple the emitting layer with the pre-stretched elastomeric adhesive (VHB 4905). This hybrid device, featuring an ultrathin LED structure (<3 µm), achieved a CE of up to 9.2 cd A⁻¹, which is 70% higher than that of control devices fabricated on rigid ITO/glass substrates. The device maintained stable luminance and CE under strains ranging from 0%

to 20% over multiple cycles. After 1000 consecutive stretch-release cycles, the brightness decreased by only 25%, while the CE increased by 25% compared to the initial value (Fig. 3b). Zhao et al. 60 developed a highly FLED that incorporates a AgNW-based polymer electrode as the anode and MAPbBr₃ as the emissive layer. This innovative device exhibits exceptional mechanical flexibility and strength while maintaining performance integrity. It can bend to a radius of 2.5 mm and endure 1000 bending cycles between a flat state and a 4 mm bending radius without any significant degradation in performance (Fig. 3c).

Leveraging excellent conductivity, thermal conductivity, and flexibility, MXene composite electrodes not only optimize charge transport but also significantly improve the device's heat dissipation capabilities, thereby enhancing long-term stability. Cao et al. extensively explored the application of MXene composite electrodes in flexible PeLEDs⁶¹. They utilized a mixture of silver nanoparticles (AgNPs), AgNWs, MXene, and Poly(3,4-ethylenedioxythiophene): poly(styrenesulfonic acid) (PEDOT:PSS) as a hybrid composite material, optimizing charge transport and reducing interface resistance, which effectively improved the device's efficiency and stability. Fig. 3di shows that the MXene composite electrodes significantly outperform traditional electrodes in terms of heat dissipation performance, thereby contributing to the long-term operational capability of flexible devices. Fig. 3dii presents a photo of a large-area flexible PeLED device operating at 5 V after assembly, validating the effective application of MXene composite electrodes in large-size and flexible devices, indicating that the electrode material can maintain stable performance while ensuring high luminous efficiency.

Seo et al. exploited graphene, which possesses high flexibility and superior properties, as an anode to achieve high-performance flexible

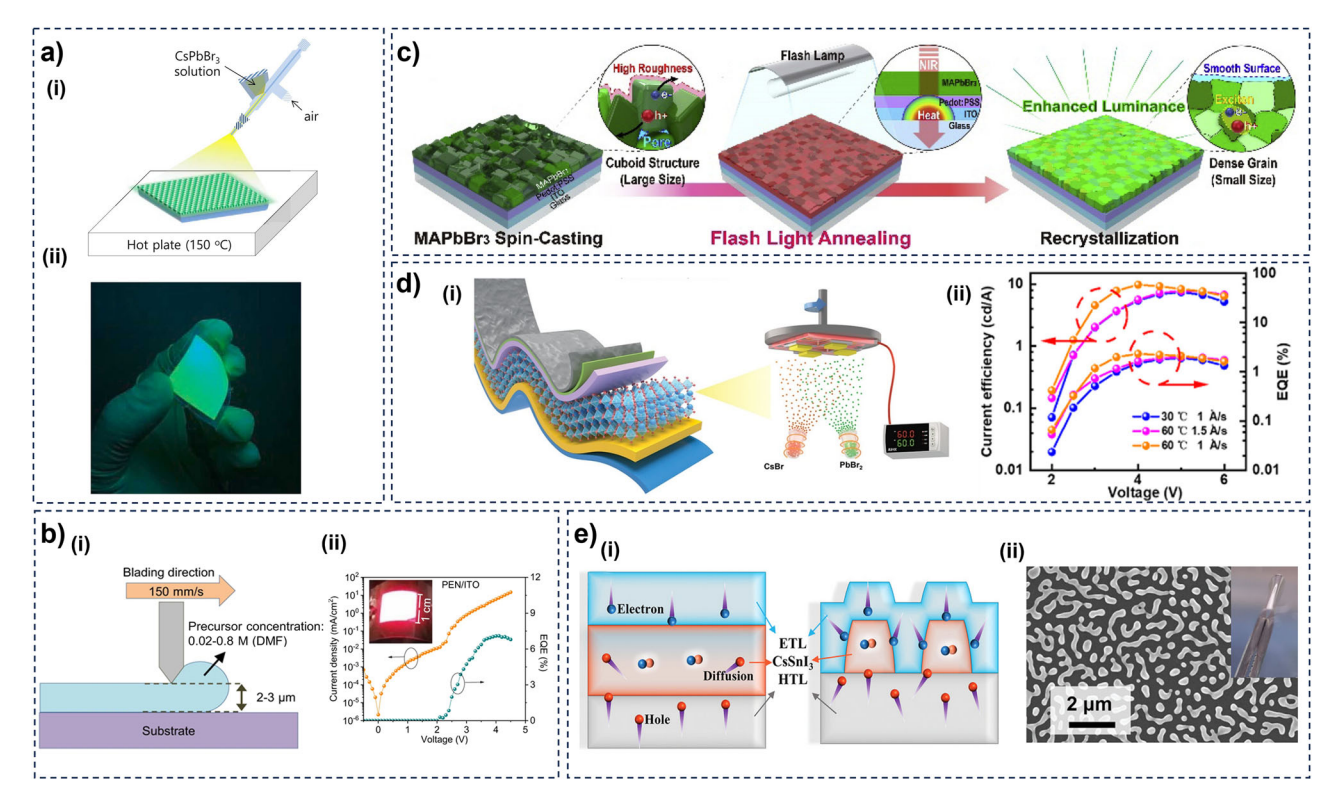


Fig. 4 | **3D perovskite thin films-based flexible PeLEDs. a** Schematic illustration of spray-coating process (i) and polymer substrate-based flexible large-area PeLED (ii). Reproduced with permission from ref. **63**. Copyright 2022, Elsevier. **b** The process of the doctor-blading (i) and current density and EQE curves of doctor-bladed PeLEDs (ii). Under the terms of Creative Commons Attribution International License (CC-BY 4.0). c Schematic illustrations of the flash-induced ultrafast recrystallization of perovskite (MAPbBr₃). Reproduced with permission from ref. **67**. Copyright 2019, Elsevier. **d** Schematic diagram of the CsPbBr₃ layer thermal vacuum co-evaporation

deposition process in conjunction with in situ dynamic thermal crystallization (i), and CE and EQE curves of PeLED devices with CsPbBr₃ film emitter layers prepared at different substrate temperatures and deposition rates with respect to applied bias voltage. Reproduced with permission from ref. 69. Copyright 2020, American Chemical Society. e Schematic illustration of the charge carriers transport and recombination process in the PeLEDs based on flat and dendritic CsSnI₃ film (i) and SEM images of dendritic CsSnI₃ films after 2000 cycles bends (ii). Reproduced with Permission from ref. 70. Copyright 2021, John Wiley and Sons.

devices⁶². As illustrated in Fig. 3e, the graphene electrode mitigated exciton quenching, typically caused by metal atom species diffusing from ITO into the buffer hole-injection layer (Buf-HIL). Consequently, the Gr-PeLEDs (PeLEDs with a graphene anode) showed a high $\rm CE_{max}$ of 16.1 cd $\rm A^{-1}$ and maximal luminance (L_{max}) of nearly 13,000 cd m⁻², with the current density only decreasing slightly to ~81% of its initial value after 1200 bending cycles.

In summary, the selection of substrates and electrodes with enhanced flexibility, transparency, and stability is of paramount importance for improving the performance of flexible PeLEDs. Flexible substrates must not only exhibit mechanical robustness and flexibility but also possess thermal stability to withstand the processing conditions and operational demands. For the electrodes, a delicate balance between conductivity and transparency is crucial, especially for the bottom electrodes, whose functions align in both carrier injection and light extraction. For the top electrode, maintaining high conductivity under various bending conditions is essential. Soft metals such as aluminum (Al) and silver (Ag), as well as nanostructured metal patterns like ultrathin gold films, are effective choices due to their excellent mechanical flexibility and electrical conductivity.

Moreover, improving the conductivity of flexible electrodes is vital for efficient carrier transport, which directly impacts the device efficiency. Efficient carrier transport minimizes non-radiative recombination and ensures better charge balance, leading to reduced efficiency roll-off and enhanced operational stability. By employing these optimized substrates and electrodes, flexible PeLEDs can achieve significantly higher brightness, EQE, and operational lifetime, making them more viable for practical applications.

Beyond the strategies applied to flexible substrates and electrodes, the intrinsic properties of the perovskite emitting layer are significant limiting

factors for enhancing the performance of flexible LED devices. The initial perovskite materials utilized in flexible PeLEDs were 3D perovskites, which have been extensively studied and applied due to their promising optoelectronic properties and solution processability. In the next section, we will discuss the advancements in flexible PeLEDs based on 3D perovskite thin films.

3D perovskite thin films-based flexible PeLEDs

Conventional methods for preparing the perovskite layer in 3D perovskite thin films-based flexible PeLEDs are primarily categorized into solution-processing and thermal evaporation techniques. For instance, Park et al. utilized a spray-coating method to fabricate large-area flexible PeLEDs, achieving a $L_{\rm max}$ of 17,795 cd m $^{-2}$ and an EQE $_{\rm max}$ of 6.18% (Fig. 4a) 63 . During the deposition of metal halide perovskites, whether through solution processing or thermal evaporation, the primary goal is to achieve uniform thin films with broad coverage and no pinholes. This uniformity is crucial for minimizing steric hindrance and avoiding the formation of shunt channels, which enhances the overall efficiency of the device 2 . Ongoing advancements in preparation techniques continue to drive improvements in the performance of perovskite-based devices.

Traditional techniques, such as spray-coating and blade-coating, often face challenges in precisely controlling the surface morphology and thickness of perovskite films, which limits the EQE of the resulting devices 64 . To address these limitations, Chu et al. introduced a low-temperature doctorblading technique (Fig. 4bi) for fabricating large-area perovskite films with high uniformity and smoothness 65 . By employing an ultrafast coating speed of $150~{\rm mm~s^{-1}}$, a low processing temperature of 50 °C, and a nitrogen knife pressure of 0.2 MPa, they reduced film roughness from 394.7 nm to 0.8 nm

using a 0.02 M FPMAI (4-fluorophenylmethylammonium iodide) precursor solution. This optimized process enabled PeLEDs to achieve an EQE of 7.1% for a 1 cm² device (Fig. 4bii), with uniform emission over a 28 cm² area, providing a cost-effective method for fabricating the emissive layer.

The solution-processing method for fabricating perovskite layers typically requires a thermal annealing step, which consumes significant time and energy. Additionally, this step may introduce high roughness and defects due to the inherent limitations of the self-assembly process used in solution coating⁶⁶. Junk et al. introduced a flash lamp annealing (FLA) technique (Fig. 4c) to achieve ultrafast recrystallization of the perovskite (MAPbBr₃) active layer in PeLEDs⁶⁷. This process transforms the perovskite from a cubic to a densely recrystallized morphology with 38 nm grains, enhancing radiative recombination and reducing surface roughness by 62%. Consequently, the flexible PeLEDs fabricated using FLA exhibited a performance improvement of 252% over devices processed by conventional heat annealing. Liu et al. utilized inkjet printing to fabricate large-area (28 cm²) red PeLEDs on flexible substrates, achieving an EQE of 14.3% with a mixed FA_{0.8}Cs_{0.2}PbI₃ perovskite composition⁶⁸.

Beyond the limitations of the self-assembly process, solution-processed perovskites often produce uneven films due to low solubility in organic solvents. Therefore, the thermal co-evaporation method, capable of overcoming these limitations, has been widely employed in the research and fabrication of flexible 3D PeLEDs. Chen et al. systematically investigated the morphology and crystallization process of inorganic CsPbBr₃ perovskite layer films fabricated by thermal co-evaporation, in conjunction with continuous low-temperature thermal annealing to promote in situ dynamic thermal crystallization (Fig. 4di)⁶⁹. The optimized flexible CsPbBr₃ LEDs exhibited an impressive luminance of ~17,350 cd m⁻² at 6.5 V (Fig. 4dii), with a maximum CE of ~10.3 cd A⁻¹, and excellent stability, with a half-lifetime exceeding 400 minutes when the initial luminance was 500 cd m⁻².

In the 3D perovskite structure, the A-site cations (e.g., MA⁺ or FA⁺) form weak hydrogen bonds with the inorganic framework (BX₆⁴⁻ octahedra), resulting in insufficient rigidity of the overall framework. Additionally, the inorganic framework in 3D structures extends in all directions and lacks the buffering and protective organic layers found in 2D perovskites. This makes 3D perovskites more prone to deformation or damage under stress. By improving the microstructure of perovskite films, grain boundary defects are reduced, and the mechanical properties and charge transport characteristics of the films are optimized, thus providing high-quality active layers for flexible PeLEDs. As shown in Fig. 4e, Lu et al. prepared dendritic CsSnI₃ films using a solution process, which exhibited a unique morphology and mechanical properties, with a tree-like micro-nano structure on the surface that optimized the balance between hole and electron injection, reduced non-radiative recombination, and enhanced radiative recombination efficiency⁷⁰. Flexible near-infrared (NIR) PeLEDs achieved an EQE of 5.4%, retaining 93.4% of their initial efficiency after 2000 bending cycles. The morphological characteristics of these films contribute to improved crack resistance and deformation tolerance, offering an effective strategy for enhancing flexibility.

Although tremendous progress has been made in flexible PeLEDs based on 3D perovskite thin films, their inherent instability remains a critical barrier to industrialization and commercialization. Consequently, regulating dimensionality to enhance device lifetime has garnered increasing attention as a promising avenue for research and development. Essentially, low-dimensional perovskites involve 2D, 1D, and 0D structures. The dimensionality reduction of perovskite materials can typically be achieved at both the morphological and molecular levels. In terms of morphological regulation, common low-dimensional perovskite structures include 2D nanoplatelets, 1D NWs and nanorods (NRs), as well as 0D QDs. At the molecular level, the application of appropriate organic ligands can further refine 3D perovskite structures into lower dimensions. For both morphological and molecular dimensionality control, this reduction in size leads to stronger quantum confinement effects. These effects are highly beneficial for enhancing PLQY and improving overall optoelectronic performance⁷¹.

Low-dimensional perovskite-based flexible PeLEDs

Molecular-level 2D perovskites are more widely adopted in flexible PeLEDs compared to their morphological-level counterparts. In these structures, various ammonium ligands are employed to form spacer layers that sandwich the perovskite octahedral units⁷². The mechanical properties of 2D perovskites are superior to those of 3D perovskites, primarily due to their unique layered structure and material characteristics^{41,73}. These layered structures allow for interlayer sliding under external forces without compromising the overall framework, while the organic layers act as buffers to effectively disperse stress^{74–76}. Furthermore, the mechanical properties of 2D perovskites can be further optimized by adjusting the thickness of the inorganic layers (i.e., reducing the n value) and varying the lengths of the organic cation chains. Long-chain organic cations significantly reduce Young's modulus, resulting in greater flexibility and improved crack resistance⁷⁷. These features endow 2D perovskites with exceptional mechanical stability, making them highly promising for flexible optoelectronic devices

Similar to flexible 3D PeLEDs, spin-coating is the preferred preparation method in 2D and quasi-2D PeLEDs research due to its simplicity, low equipment requirements, and capability to produce high-quality films⁷⁸. However, spin-coating faces challenges in large-area flexible PeLEDs due to difficulties in ensuring film uniformity and controlling film thickness. Alternatively, inkjet printing is another important thin-film fabrication technique that can uniformly coat 2D and quasi-2D perovskite solutions onto large-area flexible substrates by precisely controlling the liquid ink ejection nozzles^{79,80}. For instance, Vescio et al. demonstrated inkjet-printed lead-free PEA₂SnI₄-based flexible PeLEDs⁸¹, achieving a maximum EQE of 1% (Fig. 5a), thereby showcasing the wide applicability and environmental friendliness of inkjet printing on various substrates.

Another unique strategy for 2D perovskites involves regulating the distribution of n-values to enhance light emission performance and improve device design flexibility^{82,83}. Rui et al. explored a strategy for optimizing the optoelectronic performance of quasi-2D perovskites by adjusting the quantum well thickness, emphasizing the role of quantum wells in light emission⁸⁴. Consequently, the n = 2 device exhibited optimal performance, achieving a maximum brightness of 212 cd m⁻², a CE of 0.44 cd A⁻¹, and an EQE of 0.148%, attributed to its enhanced quantum confinement and exciton radiative recombination.

Cheng et al. enhanced the efficiency of 2D PeLEDs through morphological control⁸⁵. Polyethylene glycol (PEG), a Lewis base with superior solubility and rheological properties, interacts chemically with Lewis acidic Pb²⁺, facilitating strong passivation of grain boundaries and reducing nonradiative recombination in perovskites. Additionally, PEG serves as a matrix that regulates the growth of perovskite crystal grains, fostering uniformity in perovskite thin films and significantly reducing pinhole density. This synergistic effect enables precise morphological control, resulting in perovskite films with high surface coverage, suppressed current leakage, and improved electron-hole balance, thereby enhancing radiative recombination efficiency. Notably, this strategy is scalable to flexible substrates, achieving highly efficient flexible PeLEDs with a competitive CE of 31.0 cd A⁻¹ (Fig. 5b).

Compared to their 3D and 2D counterparts, current research on 1D and 0D flexible PeLEDs is primarily focused at the molecular level. For instance, 1D perovskite NWs and NRs possess a unique grain boundary-free morphology that demonstrates exceptional optical and electrical properties, including long charge-carrier diffusion lengths and lifetimes, efficient carrier transportation along their axis, and highly anisotropic polarization effects^{86–90}. Meanwhile, the strong spatial confinement of carriers in the radial direction and the formation of self-trapped excited states lead to substantial Stokes shifts^{91–93}, enabling high PLQY values and superior display performance. Moreover, the excellent mechanical properties of NWs make them ideal candidates for flexible optoelectronics. 1D NWs-based flexible PeLEDs have shown impressive performance in terms of EQE, bending radius, and bending cycles. For instance, Zhang et al. fabricated perovskite NWs in porous alumina templates via a capillary effect⁹⁴. These

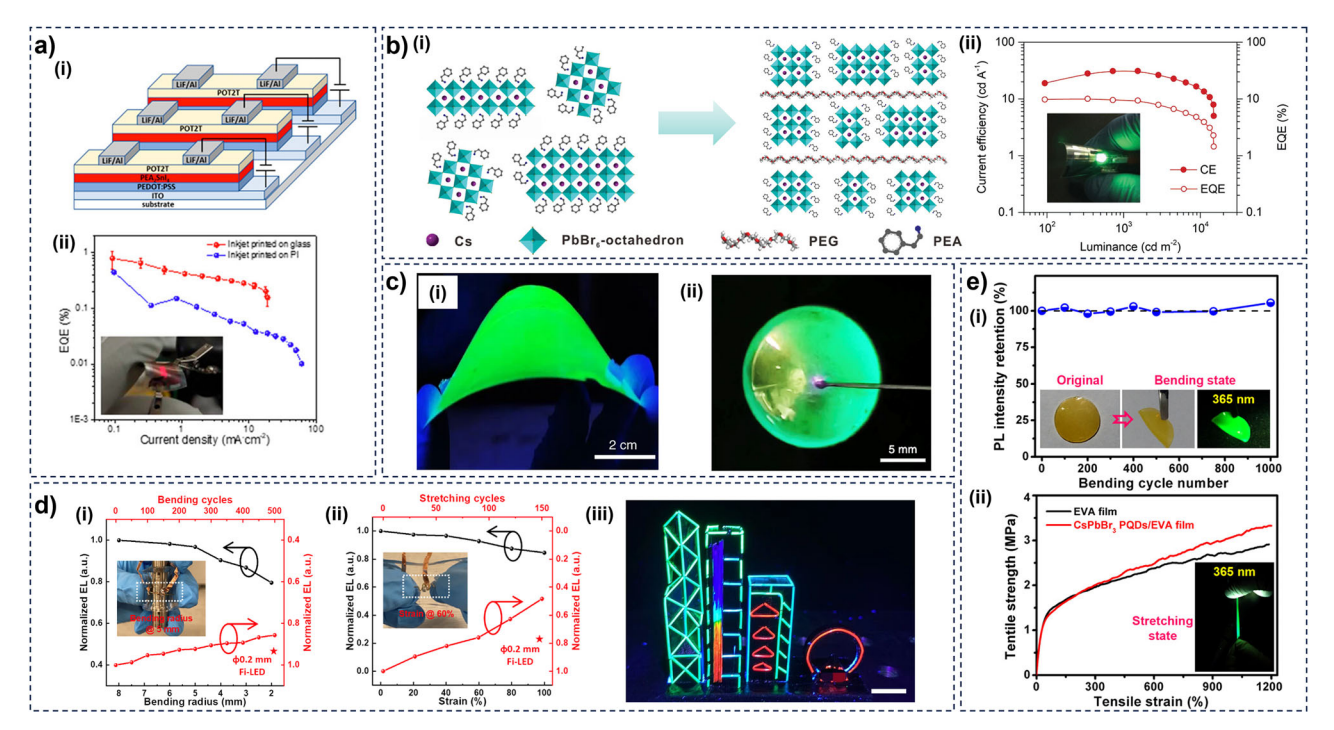


Fig. 5 | Low-dimensional flexible PeLEDs. a Device structure (i) and EQE vs current density (ii) of 2D PEA $_2$ SnI $_4$ inkjet-printed LEDs. Under the terms of Creative Commons Attribution International License (CC-BY 4.0). **b** Schematic mechanism of the perovskite morphology control with the PEG (i), and CE and EQE as a function of luminance (ii). Reproduced with permission from ref. 85. Copyright 2019, John Wiley and Sons. **c** Fluorescent photographs of four-inch wafer-scale MAPbBr $_3$ QWs on Corning Willow glass (i), and EL image of a 3D spherical device under 10 V bias (ii). Reproduced with permission from ref. 95. Copyright 2022,

Springer Nature. **d** Bendability (i) and stretchability (ii) characterizations, and (iii) Victoria Harbor built by mounting batches of fibers. The unlabeled scale bar is 1 cm. Under the terms of Creative Commons Attribution International License (CC-BY 4.0). **e** PL intensity retention of the EVA-160 film after repeatedly bending for 0–1000 cycles (i), and tensile curves of the pure EVA film and EVA-160 film (ii). Reproduced with permission from ref. 104. Copyright 2018, American Chemical Society.

NWs demonstrated high density and good crystallinity, resulting in a 45% improvement in device EQE, from 11% to 16%, compared to the planar control device. Importantly, the device maintained 86% of its luminance even under a 180° bend and retained 25% of its original luminance after 500 bending cycles, while the planar control device ceased operation after just 150 cycles.

By reducing the NWs' diameter to a size comparable to the exciton Bohr radius, Zhang et al. employed perovskite quantum wires (QWs) grown via a close-spaced vapor reaction (CSVR) in porous alumina templates to yield PeLEDs with high performance and stability⁹⁵. The quantum confinement effect, combined with the passivation from the porous alumina templates, results in a significantly improved radiative recombination rate and a state-of-the-art PLQY of 92%. Additionally, the hydrophobic porous alumina templates provide excellent stability, with a PL lifetime (T_{PL50}) of over 5644 h. This growth method also exhibits high potential for scalability, and the perovskite QWs grown in porous alumina templates demonstrate good flexibility, as evidenced by PL images on a 4-inch flexible substrate (Fig. 5ci). High-performance top-emitting PeLEDs have been achieved with a maximum EQE of 8.6% by applying transparent IZO electrodes. Furthermore, the use of ultrathin Au electrodes yielded a flexible PeLED device with an area of ~7 cm². A 3D spherical LED device with excellent luminance uniformity has also been fabricated (Fig. 5cii), demonstrating the feasibility of CSVR-grown perovskite QWs for diverse lighting and display applications.

Utilizing porous alumina templates with ultra-small pore sizes (~6.4 nm diameter), Cao et al. fabricated high-efficiency perovskite QWs-based PeLEDs. They employed 1,3,5-tris(bromomethyl)-2,4,6-triethylbenzene (TBTB)-doped 1,1-Bis[(di-4-tolylamino)phenyl]cyclohexane (TAPC) as a passivation layer, where TAPC passivated surface defects and facilitated carrier transportation, while TBTB provided a Br-rich environment to fill Br vacancies. Additionally, 1,4,5,8,9,11-Hexaazatriphenylenehexacarbonitrile

(HAT-CN) was thermally deposited to serve as both a hole-injection layer and a buffer layer. Consequently, the top-emitting devices with the structure of Al/aluminum oxide (Al $_2$ O $_3$)/perovskite QWs/TAPC/HAT-CN/ITO have shown remarkable EQE values of 12.41%, 16.49%, 26.09%, and 9.97% for blue, sky-blue, green, and pure-red emission regions, respectively. Moreover, the perovskite QWs-based flexible devices have demonstrated uniform luminance under bending, highlighting the versatility of perovskite QWs for future applications.

Khan Lê et al.⁹⁷ synthesized perovskite nanofibers through a one-step fabrication process, showcasing the potential of fiber PeLEDs. Subsequently, Ren et al. 98 developed all-organic perovskite QWs-based fiber LEDs using porous alumina templates on Al fibers. Through anion exchange treatment, full-color emission (green, blue, and red) was achieved. The encapsulation of porous alumina templates and Al fibers imparted excellent bendability and stretchability to the devices. As shown in Fig. 5di, ii, after bending with a radius of 2 mm, the electroluminescence (EL) intensity remained at 80% of its initial value, while after 500 bending cycles with a bending radius of 5 mm, the device retained over 85% of its initial EL intensity. Furthermore, the device maintained 85% of its luminance under 100% strain. The flexibility of perovskite QWs-based fiber LEDs allows for diverse shapes, Fig. 5diii shows "Victoria Harbor" structure created from various types of perovskite QWs. The results reviewed in this section clearly highlight the promising potential of 1D perovskite NWs and QWs for flexible display and lighting applications.

0D QD-based flexible PeLEDs also demonstrate immense potential in flexible optoelectronic technologies due to their exceptional optical properties and fabrication flexibility 59,99 . The luminous characteristics of PeLEDs stem from the quantum confinement effect of perovskite QDs (PQDs), resulting in ultra-narrow emission linewidths (γ -values) typically less than 20 nm and tunable emission wavelengths 100 , ensuring high color purity across the visible spectrum. Coupled with PLQYs exceeding 90%, QD

PeLEDs hold significant promise for applications in high-end displays and lighting devices ^{12,92,101,102}. Moreover, PQD materials can be fabricated using straightforward solution processes under ambient conditions, allowing compatibility with flexible substrates such as plastics and polymer films. Thus, PQDs lay a solid foundation for mechanical flexibility in devices ¹⁰³.

Compared to QDs in solution, gel-based composites retain their structure without shrinkage and exhibit superior stability. Chen and collaborators prepared color conversion films made from CsPbBr₃ PQDs and ethylene-vinyl acetate copolymer (EVA), achieving a PLQY as high as 40.5%¹⁰⁴. As shown in Fig. 5ei, CsPbBr₃ PQDs/EVA films demonstrate impressive flexibility, continuing to emit a vibrant green glow under UV light (365 nm), even when bent to an extreme angle of 180°. Notably, after undergoing 0 to 1000 bending cycles, no decrease in PL intensity was observed, largely due to the inherent flexibility of the EVA matrix. Moreover, tensile test results (Fig. 5eii) confirmed that EVA-160 films, with a mass ratio of CsPbBr₃ PQDs to EVA of 0.6, exhibit mechanical behavior similar to that of pure EVA films. When stretched to 350% of their original length, these films maintain steady emission under UV light, showcasing their exceptional mechanical and optical properties.

Sun et al. developed free-standing, flexible CsPbX₃ QD soft gels, scaled at 10×19 cm², through the self-hydrolysis of coordinating silane¹⁰⁵. A flexible white LED was fabricated by directly placing thin red and green gels onto a transparent substrate, achieving chromaticity coordinates of (0.30, 0.32) and a color temperature of 7161 K, as well as a color gamut exceeding 128% of the NTSC standard, surpassing previous powder-based products. Advantages of these devices include simple fabrication processes and highlight conversion efficiency, making them suitable for large-area flexible displays and applications requiring robust environmental tolerance.

Through an interface engineering approach combining inkjet printing and plasma etching, bright and uniform red, green, and blue (RGB) micro-PeLED arrays with pixel sizes as small as 45 µm have been successfully fabricated. The integration of flexible device technology with RGB micro-PeLED arrays, showcasing EQEs of 0.832%, 0.419%, and 0.052% for RGB emissions, respectively, has enabled the fabrication of flexible displays with a resolution of 210 pixels per inch¹⁰⁶. Electroluminescent QD PeLEDs exhibit high efficiency, low driving voltage, and extensive potential for device integration, making them increasingly valuable for applications in flexible displays and wearable smart devices⁴.

Despite the improvements in optoelectronic performance achieved through dimensionality regulation, simultaneously obtaining devices that feature both high performance and mechanical properties remains a challenge. A promising approach to address this issue is to combine a high-performance perovskite layer with polymers that possess excellent flexibility.

Perovskite/polymer composites-based flexible PeLEDs

Young's modulus, a critical parameter for evaluating the mechanical properties of materials, has been theoretically and experimentally reported for metal halide perovskites to range from 12 to 20 GPa¹⁰⁷⁻¹⁰⁹. This is substantially lower than that of conventional inorganic luminescent materials, such as silicon, GaN, and GaAs, which typically exceed 100 GPa^{75,110,111}. The relatively low Young's modulus, combined with the superior ductility of perovskites, makes them highly suitable for high-performance flexible optoelectronic devices.

However, the performance of flexible PeLEDs is still compromised by prolonged mechanical deformation, such as bending and stretching. This degradation is primarily attributed to the intrinsic brittleness of perovskite materials. The tensile and compressive strains generated during bending lead to vertical cracks along the grain boundaries and facilitate film delamination from the substrate^{1,112,113}. Such vertical cracks expedite the infiltration of oxygen and moisture, consequently accelerating material degradation within the perovskite layer^{114,115}. Moreover, film delamination can result in immediate device failure.

To mitigate these issues, the development of perovskite-polymer composites has been identified as an effective strategy to enhance mechanical flexibility, resistance to deformation, and robust interfacial adhesion $^{116-118}$. For example, Zang et al. proposed an innovative self-healing strategy that involves the incorporation of a multifunctional silane molecule (3,3,3-trifluoropropyl)trimethoxysilane into the quasi-2D perovskite PEA2Csn-1PbnBr3n+1, leading to the formation of flexible Si-O-Si networks (Fig. 6a). The reversible hydrolysis and condensation reactions within this siloxane network, along with the properties of the fluorinated alkyl chains, impart exceptional self-healing capabilities to the perovskite films. As a result, the synergistic effects enabled the flexible PeLEDs to achieve an extraordinary EQE of 16.2% and retain 75% of their initial efficiency after 1000 bending cycles, demonstrating exceptional mechanical and operational stability.

Additionally, Bade et al. designed a composite structure by embedding perovskite within a poly(ethylene oxide) (PEO) matrix¹²⁰. The PEO matrix serves as an elastic connector for the brittle perovskite microcrystals, providing stretchability to the composite emissive layer. Consequently, these devices can withstand strains of up to 40% and maintain functionality over 100 stretching cycles, showcasing excellent mechanical robustness (Fig. 6b).

Sun et al. introduced a low-cost, green biomass material ethyl cellulose (EC) into CsPbI₃ nanocrystals as a cross-linking agent between adjacent halide octahedra¹²¹. As shown in Fig. 6c, the oxygen atoms in EC, particularly those in the ethyl ether groups, exhibit high electron density, which facilitates the formation of coordination bonds with undercoordinated Pb²⁺. The theoretical simulation also indicated that the formation energy of iodine vacancies increased with the EC treatment, which demonstrates the potential of EC on suppressing defect formation. Consequently, the PLQY of CsPbI₃ nanocrystals treated with EC increased significantly from 63% to 87%. Furthermore, the excellent flexibility of EC and its crosslinking effect with perovskite nanocrystals enhanced the mechanical deformation resistance of the perovskite layer. After 1000 bending cycles at a radius of 3 mm, the brightness exhibited minimal decay. Even under repeated bending with an ultra-small radius of 1 mm, the nanocrystals maintained high brightness.

Inspired by the integration of rigid scales and soft tissues in pangolins, Qian et al. developed a bioinspired structural design for self-healing flexible PeLEDs using a polymer-assisted crystallization method combined with the flexible elastomeric properties of methylene diphenyl diisocyanate-based polyurethane (MDI-PU)¹²². In such a unique design, harmful cracks can be effectively self-healed through the intramolecular and intermolecular hydrogen bonding of MDI-PU upon thermal treatment. The optimized flexible blue PeLEDs achieved a record-breaking EQE of 13.5% with exceptional bending strain resistance, retaining 87.8% and 80.7% of their initial efficiency after 2000 cycles of bending and twisting operations, respectively (Fig. 6d). Hence, as a good crosslinking agent, polymer materials can effectively improve both the mechanical and optical properties of perovskite thin films, hence leading to excellent flexibility and mechanical durability.

Therefore, integrating a flexible polymer with perovskite can effectively the performance of the flexible PeLEDs. The inherent flexibility of the polymer improves the mechanical properties and robustness of the devices, while its interaction with perovskite optimizes crystallization, reduces defect density, and regulates nucleation and growth, thereby achieving improved film uniformity and performance. Additionally, the polymer's ability to protect the perovskite layer from oxygen and moisture significantly boosts device stability and operational lifetime.

The performance of flexible PeLEDs reported recently is summarized in Table 1 to compare the capacity of different strategies.

Hence, compared with single perovskite, exploiting perovskite/polymer composites as the emitting layer for flexible PeLEDs is the approach to not only enhances the mechanical flexibility of the devices but also helps in maintaining their high optoelectronic performance. The properties of different emitting layers are summarized in Table 2.

Applications of flexible PeLEDs

Flexible PeLEDs have demonstrated significant potential for various applications as deformable optoelectronic devices, particularly in the realms

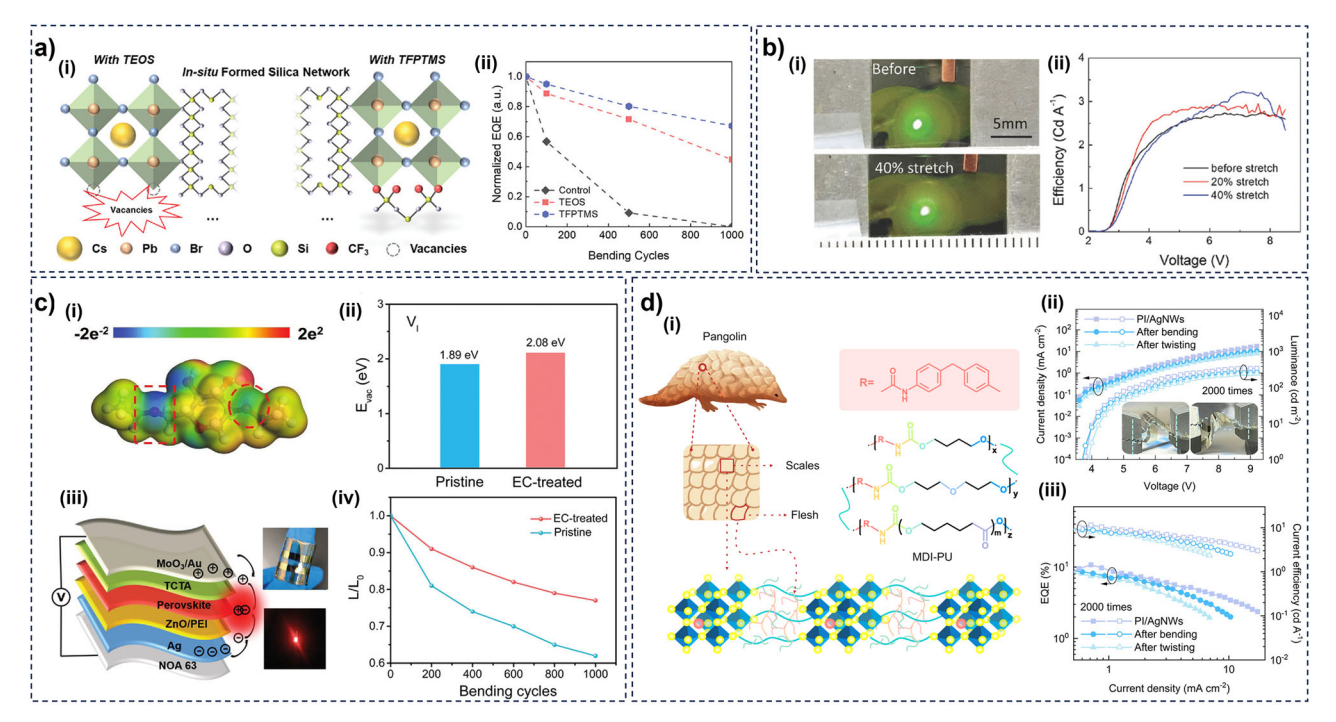


Fig. 6 | Perovskite/Polymer Composites-based Flexible PeLEDs. a Schematic illustration of the interaction between silica network with perovskite (i), bending cycles-dependent EQE degradation behavior (ii). Reproduced with permission from ref. 119. Copyright 2022, John Wiley and Sons. **b** Photos of a lit LED under a 4V bias before (top) and after (bottom) stretching to 40% strain (i) and CE-voltage characteristics of the stretchable PeLEDs before and after stretching to 20% and 40% strain (ii). Reproduced with permission from ref. 120. Copyright 2017, John Wiley and Sons. **c** Molecular structure and calculated ESP profile of a monomer molecule of

EC (i), formation energies of surface I vacancies in the perovskite without and with EC treatment (ii), schematic and digital photo of the flexible PeLEDs (iii), and luminance of the device with different bending cycles at a bending radius of 3 mm. Reproduced with permission from ref. 121. Copyright 2022, John Wiley and Sons. d Schematics of MDI-PU-incorporated flexible perovskite films (i), J-V-L characteristics (ii), and EQE and CE (iii) as a function of current density measured after repeated bending and twisting. Reproduced with permission from ref. 122. Copyright 2022, American Chemical Society.

of foldable lighting and wearable display technologies. Zhao et al. showcased large-scale flexible NIR PeLEDs suitable for medical illumination ¹²³. As illustrated in Fig. 7a, the uniform and intense emission from these devices facilitates clear visualization of even subcutaneous blood vessels. When integrated with other functional devices, this non-invasive detection capability offers a promising approach for monitoring various physiological features.

In another development, Chou et al.¹²⁴ fabricated perovskite light-emitting touch-responsive devices (LETDs) by combining perovskite with a composite electrode made of AgNW and PU for the touch interface. When pressure is applied to the device's surface, the electrode makes direct contact with the perovskite light-emitting layer, forming a Schottky contact that allows for charge transport, thus illuminating the device. Upon the release of pressure, the electrode detaches from the perovskite layer, ceasing photon emission. The flexibility of the devices enables them to adhere to curved surfaces, ensuring visual displays with good clarity, as shown in Fig. 7b. The versatility of the LETDs positions them as strong candidates for applications in biometric fingerprint recognition, motion detection, and other interactive displays.

High-quality displays are increasingly vital for wearable technology. Kwon et al. achieved ultrahigh-resolution flexible PeLEDs designed for attachable displays, as depicted in Fig. 7c¹²⁵. They developed a novel double-layer transfer printing technique to pattern the perovskite and organic charge transport layers, effectively preventing internal cracking during transfer. This innovative method yielded an ultrahigh resolution of 2550 PPI for RGB pixelated patterns and 33,000 line pairs per inch for monochromatic patterns, both with a transfer yield of 100%. The resulting ultrathin PeLEDs are capable of operating on curvilinear surfaces—such as human skin, leaves, and the edges of blades—while withstanding various mechanical deformations, including bending, folding, wrinkling, and twisting. Encapsulated with waterproof parylene on both upper and lower

surfaces, these devices exhibit excellent moisture stability. Their enhanced optical and mechanical properties make these skin-attachable PeLEDs promising for future applications in wearable devices, the Internet of Things (IoT), virtual reality (VR), and augmented reality (AR).

Shan et al. employed a hybrid strategy and a simple solution assembly process to fabricate bifunctional fibers based on PQDs, as illustrated in Fig. 7d¹²⁶. Their approach utilized a hybrid perovskite ink composed of poly[bis(4-phenyl)(2,5,6-trimethylphenyl)amine] (PTAA), 1,3,5-tri[(3pyridyl)-phen-3-yl]benzene (TmPyPB), and PQDs. Layer-by-layer, these materials were coated onto transparent PET fibers using a dip-coating process. The resulting perovskite fibers demonstrated excellent electroluminescent properties, alongside impressive photodetection capabilities. This led to the successful demonstration of a wearable light fidelity (LiFi) system utilizing the bifunctional fibers, enabling them to serve as both transmitters and receivers for true full-duplex communication. Notably, these fibers maintained functionality even at a bending radius of 4.5 mm, showcasing their flexibility. This advancement could significantly enhance data transmission rates and facilitate real-time interactions between devices, marking a critical development in smart wearable and IoT technology.

The ongoing research and exploration of applications involving flexible PeLEDs are poised to greatly enhance human life in the future. As conceptualized in Fig. 8, several scenarios depict flexible PeLEDs integrated seamlessly into daily life, including foldable screens, interactive large-area flexible displays, wearable smart electronic devices, innovative lighting systems, and advanced medical devices. These applications are not only driven by the unique material properties of perovskites but also closely intertwined with the advancements in artificial intelligence (AI) technology, which further amplifies their potential impact. We anticipate that continued research in flexible PeLED applications will yield even greater advancements in the future.

Total C.	CT Indicate and other accompany of							
rabie i į summary	Table 1 Summary of progress made on nexible Perros							
Туре	Device structure	Key improvement	EQE _{max} [%]	CE _{max} [cd A ⁻¹]	L _{max} [cd m ⁻²]	T50 [min]	Flexibility	Ref.
Flexible substrate	PEO-modified PEDOT:PSS /CH ₃ NH ₃ PbBr ₃ /PEO/PEI/AgNWs	Elastic Substrates	0.804	2.01	10227		Bending radius 2.5 [mm]	56
	Printing paper/PMMA/Ag/ZnO/PEI/Ni-doped CsPbl ₃ /TCTA/ MoO ₃ /Au	Printing paper/PMMA substrate	8.5	-	1330	-	Bending radius 3 [mm]	127
Flexible electrode	Elastomeric adhesive/AgNWs/PI composite electrode/ PEDOT:PSS/TAPC:PVK/ MAPbBr ₃ QDs/TPBi/CsF/AI	AgNWs/PI composite electrode, elastomeric adhesive	-	9.2	3187	39.6	-	59
	AgNW-polymer composite substrate/ PEDOT:PSS/PVK: TAPC/CH ₃ NH ₃ PbB _{Y3} QDs/TmPyPB/ CsF/ Al	AgNW-polymer composite electrode	2.6	10.4	1000	-	Bending radius 2.5	09
	Composite electrode/PEDOT:PSS/perovskite/TPBi/LiF/Al	MXene-Based Composite Electrodes	16.5	54.1	49807	39.6	-	61
	Four-layer graphene (4LG)/Buf-HIL (PEDOT:PSS/PFI)/ MAPbBr ₃ /TPBi/LiF /Al	Four-layer graphene electrode	3.8	18.0	≈ 13000	-	bending curvature 5–10 mm	62
3D	PFN/ITO/poly-TPD/perovskite/TPBi/LiF/Al	Blade-coating	7.1	-	-	-	-	92
	PEN/ITO/PEDOT:PSS/MAPbBr ₃ /BCP/LiF/Al	Flash light annealing		0.17	929		ı	29
	Substrate/ITO/HAT-CN/TAPC/CsPbBr-3/PO-T2T /Liq /AI	Thermal co-evaporation and low-temperature thermal annealing	-	10.3	17350	1	-	69
	PEN-ITO/PEDOT:PSS/Perovskites/B3PyMPM/LiF/Al	Dendritic lead-free PeLEDs	3.2				1	70
	PET/ITO/PEDOT:PSS/PFI/CsPbBr ₃ /TPBI/LiF/AI	Spray-coating	6.18	28.17	17795	-	bending curvature 4–12 [mm]	63
2D	PET/AgNWs/PEDOT:PSS/CsPbBr3 perovskite/TPBi/LiF/Al	Synergetic morphology control	10.1	31			1	85
	PEN/PEDOT:PSS(Ph1000) /quasi-2D perovskites/TPBi/LiF/Al	Encapsulation growth	12.8	47.1	8300		1,5,10 [mm]	128
1D	AI/Al ₂ O ₃ /PeQWs/TAPC/Au	Full-color fiber LED	15.2	-	-	-	2–8 [mm]; 500 cycles	86
	AI/AI ₂ O ₃ /CsPbBr ₃ QWs/NiO _x /IZO	3D spherical perovsite LEDs	8.76		1300		ı	96
	ITO/ PEDOT:PSS/MABr modified CsPbBr ₃ NW/TPBi/LiF/Ag	The efficiency of light extraction is improved	16		12016	37	0-180°, 500 cycles	94
Perovskite/polymer	PEN-ITO/TFB/PVK/TPBi/LiF/Al	Self-healing	16.2	-	11353	-	5[mm]	119
composites	PI/AgNWs/PEDOT:PSS/CsPb(CI/Br) ₃ /TPBi/LiF/Al	Hydrogen bond; Hotfix	13.5	-	-	-	2000 cycles	122
	PDMS/PEDOT:PSS/PEO/perovskite-PEO/ ElnGa	Stretchable PeLEDs	0.62	2.7	15,960	-	40% strain	120
	NOA 63/Ag/ZnO:PEI/Perovskite/TCTA/MoO3:Au	Reduce defect density	12.1		1674		3 [mm]	121

Summary and outlook

In conclusion, we have reviewed recent research advancements in flexible PeLEDs, with a particular emphasis on the perovskite light-emitting layer. Our analysis began by examining the progress made in developing flexible PeLEDs utilizing flexible substrates and electrodes. We categorized various perovskite materials, including 3D thin films, 2D/quasi-2D films, 1D NWs, 0D QDs, and perovskite/polymer composites, discussing their synthesis methods, optical and mechanical properties, and applications in flexible PeLEDs. The unique material properties and excellent device performance highlight the potential of flexible PeLEDs as candidates for next-generation flexible and wearable optoelectronic devices. However, further improvements in device performance are essential before these technologies can be applied in practical scenarios, which can be achieved through innovations in both perovskite materials and device structures.

Mechanical robustness is a critical challenge for the practical deployment of flexible PeLEDs, as these devices must endure various deformations, including bending, stretching, and abrasion. To address this, a rational design approach to the device structure is effective. This may involve

Table 2 | Comparisons of emitting layers of flexible PeLEDs

Emitting layer	Advantages	Disadvantages
3D perovskite	High luminance	Low PLQY, low stability, low flexibility
Low-dimensional perovskite	High PLQY, high stability	Low luminance
Perovskite/polymer composites	High PLQY, high stability, high flexibility	Poor interface contact

utilizing mechanically stable substrates and electrodes and optimizing interfacial layers to enhance adhesion between different layers. Moreover, regulating the composition and dimensionality of the perovskite emitting layer offers versatile opportunities to enhance flexibility. Incorporating perovskite/polymer composites with effective cross-linking strategies, refined polymer-perovskite interfaces, and novel self-healing mechanisms are promising methods to simultaneously achieve high performance and flexibility in flexible PeLEDs. These advancements not only address the intrinsic brittleness of perovskite materials but also pave the way for durable and reliable flexible optoelectronic devices. Beyond good flexibility, enhancing the performance of flexible PeLEDs is crucial for their industrial viability, positioning advanced additive engineering as a potential direction for future exploration.

Operational stability remains a significant obstacle, affecting both flexible and rigid PeLEDs. Non-radiative recombination due to defects on the crystal surface and grain boundaries is a primary factor that severely undermines operational stability. To combat this issue, developing rational designs for effective passivation strategies that significantly reduce defect densities within the perovskite layer is essential. Furthermore, unbalanced charge injection and transport can result in Joule heating, further exacerbating low operational stability in PeLEDs. Thus, optimizing charge transport layers to achieve balanced carrier transport is a key strategy for enhancing the durability of PeLED devices. The implementation of encapsulation strategies is also critical to mitigate the sensitivity of perovskite materials to oxygen and moisture, which can lead to degradation. Addressing these challenges will facilitate significant advances in improving the operational stability and lifespan of PeLEDs.

Another major obstacle to the practical application of flexible PeLEDs is their toxicity. Presently, high-efficiency PeLEDs are primarily based on Pb

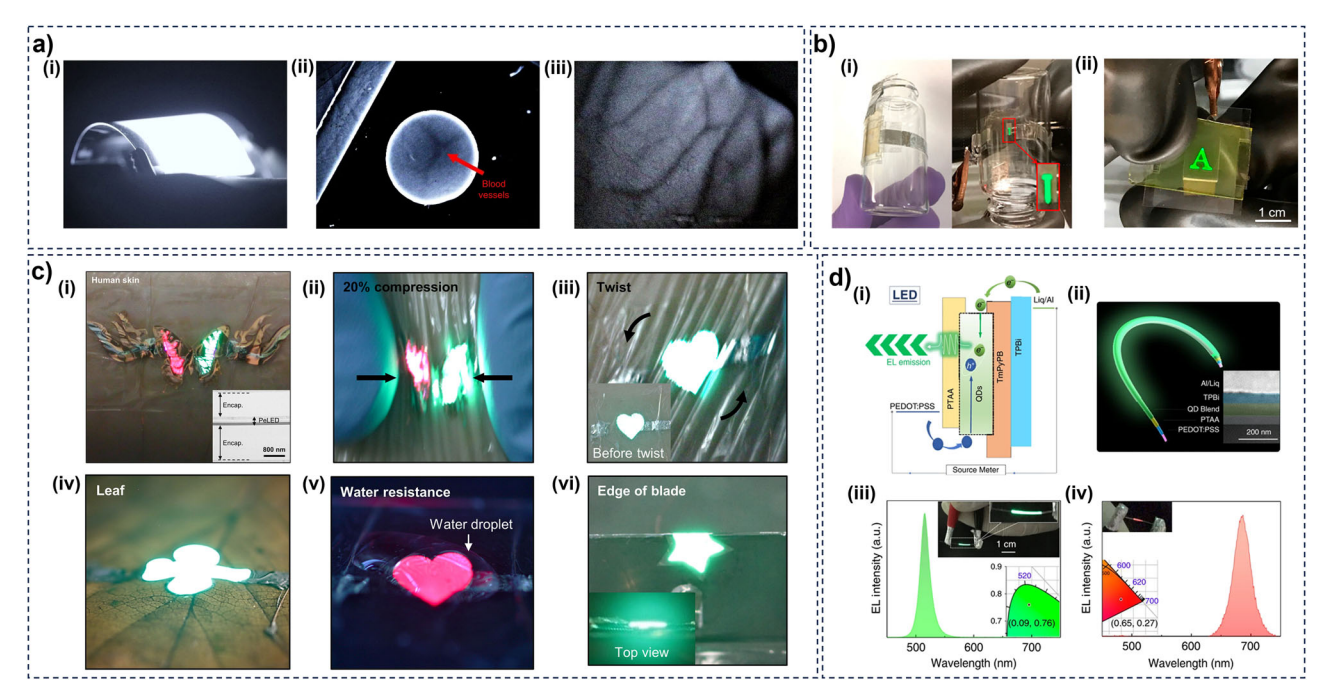


Fig. 7 | Applications of flexible PeLEDs. a NIR photographs of the large-area flexible PeLED (i), PeLED with a 0.5-inch circular window illuminating subcutaneous blood vessels on the human palm while in close contact (ii), and PeLED illuminating the back of a human fist (iii). Reproduced with permission from ref. 123. Copyright 2020, Springer Nature. b Transparent flexible LETD wrapped to a 1 in. diameter vial and glowing in the form of letter "T" when stamped (i), and photograph of a LETD under 4 V bias when an "A"-shape stamp is pressed onto the surface of the AgNW–PU top electrode (ii). Reproduced with permission from ref. 124. Copyright 2017, American Chemical Society. c Photograph of ultrathin multicolor PeLEDs attached to human skin (i), ultrathin PeLEDs attached to human

skin under various deformations: 20% compression (ii) and twist (iii), ultrathin PeLEDs laminated on a leaf (iv), demonstration of the water resistance of ultrathin PeLEDs (v), and photograph of an ultrathin PeLED folded on a razor blade edge (vi). Under the terms of Creative Commons Attribution International License (CC-BY 4.0). d Schematic illustration of the working mechanism (LED mode) of the lightemitting/detecting bifunctional perovskite fiber (ii), schematic of the structure of a perovskite EL fiber (ii), EL spectra of a green (iii) and a red (iv) electroluminescent perovskite fiber. Under the terms of Creative Commons Attribution International License (CC-BY 4.0).

Fig. 8 | Future scenarios of the applications of flexible PeLEDs. a Smart glasses, b Healthmonitoring fabric display, c Smart watches, d Foldable electronics, e Interactive large-area flexible display, f Lighting system.



compositions, which do not meet the safety standards necessary for commercialization. While alternative metal ions, such as tin (Sn), have been explored as substitutes for Pb in rigid PeLEDs, research on Pb-free flexible PeLEDs is still limited. Thus, developing high-performance, non-Pb FLEDs is a promising direction for future research and innovation.

In summary, while substantial achievements have been made concerning rigid PeLEDs, including enhanced device EQE and luminescence, the development of high-performance flexible PeLEDs lags behind. Overcoming challenges related to mechanical flexibility, operational stability, and material toxicity is critical for the future advancement and commercialization of flexible PeLEDs in wearable and other optoelectronic applications.

Data availability

No datasets were generated or analyzed during the current study.

Received: 28 January 2025; Accepted: 7 April 2025; Published online: 21 April 2025

References

- Jang, J. H., Li, S., Kim, D. H., Yang, J. & Choi, M. K. Materials, device structures, and applications of flexible perovskite light-emitting diodes. *Adv. Electron. Mater.* 9, 2201271 (2023).
- Jia, P. et al. Recent advances in flexible perovskite light-emitting diodes. Adv. Mater. Interfaces 8, 2100441 (2021).
- Zhang, Y., Khan, S. A., Luo, D. & Li, G. Flexible perovskite lightemitting diodes for display applications and beyond. *J. Semicond.* 45. 051601 (2024).
- Choi, M. K., Yang, J., Hyeon, T. & Kim, D.-H. Flexible quantum dot light-emitting diodes for next-generation displays. *npj Flex. Electron.* 2, 10 (2018).
- Gustafsson, G. et al. Flexible light-emitting diodes made from soluble conducting polymers. *Nature* 357, 477–479 (1992).
- Chang, S. et al. Flexible and stretchable light-emitting diodes and photodetectors for human-centric optoelectronics. *Chem. Rev.* 124, 768–859 (2024).
- Hua, Q. & Shen, G. Low-dimensional nanostructures for monolithic 3D-integrated flexible and stretchable electronics. *Chem. Soc. Rev.* 53, 1316–1353 (2024).
- Chwang, A. B., Hack, M. & Brown, J. J. Flexible OLED display development: strategy and status. J. Soc. Inf. Disp. 13, 481–486 (2005).

- 9. Liu, Y. F., Feng, J., Bi, Y. G., Yin, D. & Sun, H. B. Recent developments in flexible organic light-emitting devices. *Adv. Mater. Technol.* **4**, 1800371 (2019).
- Bauri, J., Choudhary, R. B. & Mandal, G. Recent advances in efficient emissive materials-based OLED applications: a review. *J. Mater. Sci.* 56, 18837–18866 (2021).
- Yadav, S., Mittal, P. & Negi, S. Recent advancements over a decade for organic light-emitting diodes: from structural diversity, role of layers, colour emission, material classification, performance improvement, fabrication to applications. *Bull. Mater. Sci.* 45, 109 (2022).
- Huang, C.-Y. et al. Inorganic halide perovskite quantum dots: a versatile nanomaterial platform for electronic applications. Nanomicro Lett. 15, 16 (2022).
- 13. Liu, Z. et al. Micro-light-emitting diodes with quantum dots in display technology. *Light. Sci. Appl.* **9**, 83 (2020).
- Guan, X. et al. Targeted elimination of tetravalent-Sn-induced defects for enhanced efficiency and stability in lead-free NIR-II perovskite LEDs. Nat. Commun. 15, 9913 (2024).
- Luo, J. et al. Efficient and stable emission of warm-white light from lead-free halide double perovskites. Nature 563, 541–545 (2018).
- 16. Li, M. et al. Acceleration of radiative recombination for efficient perovskite LEDs. *Nature* **630**, 631–635 (2024).
- Kong, L. et al. Fabrication of red-emitting perovskite LEDs by stabilizing their octahedral structure. Nature 631, 73–79 (2024).
- Meloni, S., Palermo, G., Ashari-Astani, N., Grätzel, M. & Rothlisberger, U. Valence and conduction band tuning in halide perovskites for solar cell applications. *J. Mater. Chem. A* 4, 15997–16002 (2016).
- Kim, Y.-H., Cho, H. & Lee, T.-W. Metal halide perovskite light emitters. Proc. Natl Acad. Sci. 113, 11694–11702 (2016).
- Sun, S. Q. et al. Enhancing light outcoupling efficiency via anisotropic low refractive index electron transporting materials for efficient perovskite light-emitting diodes. *Adv. Mater.* 36, 2400421 (2024).
- 21. Xiong, W. et al. Controllable p- and n-type behaviours in emissive perovskite semiconductors. *Nature* **633**, 344–350 (2024).
- 22. Chen, Z. et al. Roadmap on Perovskite light-emitting diodes. *J. Phys. Photonics* http://arxiv.org/abs/2311.11232 (2024).
- Kim, J. S. et al. Ultra-bright, efficient and stable perovskite lightemitting diodes. *Nature* 611, 688–694 (2022).

- Feng, S.-C. et al. Efficient and stable red perovskite light-emitting diodes via thermodynamic crystallization control. *Adv. Mater.* 36, 2410255 (2024).
- Gao, Y. et al. Highly efficient blue light-emitting diodes based on mixed-halide perovskites with reduced chlorine defects. Sci. Adv. 10. eado5645 (2024).
- Luo, J. et al. Vapour-deposited perovskite light-emitting diodes. *Nat. Rev. Mater.* 9, 282–294 (2024).
- Min, H. et al. Spin coating epitaxial heterodimensional tin perovskites for light-emitting diodes. *Nat. Nanotechnol.* 19, 632–637 (2024).
- Liu, H. et al. Advances and challenges in large-area perovskite lightemitting diodes. Adv. Mater. n/a, 2410154 (2024).
- Shen, Y. et al. Rational interface engineering for efficient flexible perovskite light-emitting diodes. ACS Nano 14, 6107–6116 (2020).
- Zhu, P. et al. Toward the commercialization of perovskite solar modules. Adv. Mater. 36, 2307357 (2024).
- Root, S. E., Savagatrup, S., Printz, A. D., Rodriquez, D. & Lipomi, D. J. Mechanical properties of organic semiconductors for stretchable, highly flexible, and mechanically robust electronics. *Chem. Rev.* 117, 6467–6499 (2017).
- Dunaevskiy, M. et al. Young's modulus of wurtzite and zinc blende InP nanowires. Nano Lett. 17, 3441–3446 (2017).
- Kucheyev, S. et al. Deformation behavior of ion-beam-modified GaN. Appl. Phys. Lett. 78, 156–158 (2001).
- Grillo, S., Ducarroir, M., Nadal, M., Tournie, E. & Faurie, J. Nanoindentation of Si, GaP, GaAs and ZnSe single crystals. J. Phys. D: Appl. Phys. 36, L5 (2002).
- Ott, C. et al. Flexible and ultrasoft inorganic 1D semiconductor and heterostructure systems based on SnIP. Adv. Funct. Mater. 29, 1900233 (2019).
- Zhang, Z. et al. High-brightness all-polymer stretchable LED with charge-trapping dilution. *Nature* 603, 624–630 (2022).
- Torres, J. M., Bakken, N., Stafford, C. M., Li, J. & Vogt, B. D. Thickness dependence of the elastic modulus of tris (8hydroxyquinolinato) aluminium. Soft Matter 6, 5783–5788 (2010).
- Pinto, E. et al. Transparent composites prepared from bacterial cellulose and castor oil based polyurethane as substrates for flexible OLEDs. J. Mater. Chem. C. 3, 11581–11588 (2015).
- 39. Bideau, B., Loranger, E. & Daneault, C. Comparison of three polypyrrole-cellulose nanocomposites synthesis. *J. Adv. Nanomater.***1**, 10.22606 (2016).
- Fagbohungbe, K. H., Callaway, C. P. & Risko, C. Temperaturedependent stress-strain behavior of amorphous and crystalline P3HT. J. Mater. Chem. C. 12, 19103–19115 (2024).
- Tu, Q. et al. Exploring the factors affecting the mechanical properties of 2D hybrid organic–inorganic perovskites. ACS Appl. Mater. interfaces 12, 20440–20447 (2020).
- Sun, S. et al. Factors influencing the mechanical properties of formamidinium lead halides and related hybrid perovskites. ChemSusChem 10, 3740–3745 (2017).
- Sun, S., Fang, Y., Kieslich, G., White, T. J. & Cheetham, A. K. Mechanical properties of organic–inorganic halide perovskites, CH3 NH3 PbX3 (X=I, Br and Cl), by nanoindentation. *J. Mater. Chem. A* 3, 18450–18455 (2015).
- 44. Roy, D. et al. Why does the photoluminescence efficiency depend on excitation energy in case of a quantum dot? A case study of CdSebased core/alloy shell/shell quantum dots employing ultrafast pump-probe spectroscopy and single particle spectroscopy. J. Phys. Chem. C. 123, 6922–6933 (2019).
- Needell, D. R. et al. Spectrally matched quantum dot photoluminescence in GaAs-Si tandem luminescent solar concentrators. *IEEE J. Photovolt.* 9, 397–401 (2019).
- Shen, J. et al. Exceeding 67.35% efficient and color temperature tunable white light from carbon dots with quadruple-channel

- fluorescence–phosphorescence emission. ACS Sustain. Chem. Eng. 10, 15599–15607 (2022).
- 47. Zhu, W. et al. A dual strategy to prepare CsPbBr3@ glass with a high PLQY and ultrastability: combining controllable crystallization and surface modification. *Adv. Funct. Mater.* **34.** 2408760 (2024).
- Das, S. & Samanta, A. Highly luminescent and phase-stable red/ NIR-emitting all-inorganic and hybrid perovskite nanocrystals. ACS Energy Lett. 6, 3780–3787 (2021).
- Wei, J.-H., Wang, X.-D., Liao, J.-F. & Kuang, D.-B. High photoluminescence quantum yield (> 95%) of MAPbBr3 nanocrystals via reprecipitation from methylamine-MAPbBr3 liquid. ACS Appl. Electron. Mater. 2, 2707–2715 (2020).
- Chen, S.-W. et al. Versatile deep blue fluorescent materials based on the hybridization of phenanthroimidazole and fluorene derivatives. *Dyes Pigm.* 222, 111829 (2024).
- Zhang, K., Zhu, N., Zhang, M., Wang, L. & Xing, J. Opportunities and challenges in perovskite LED commercialization. *J. Mater. Chem. C.* 9, 3795–3799 (2021).
- Liguori, R., Nunziata, F., Aprano, S. & Maglione, M. G. Overcoming challenges in OLED technology for lighting solutions. *Electronics* 13, 1299 (2024).
- Meneghini, M., Trevisanello, L. R., Meneghesso, G. & Zanoni, E. A review on the reliability of GaN-based LEDs. *IEEE Trans. Device Mater. Reliab.* 8, 323–331 (2008).
- Chen, D. et al. Ultralow trap density FAPbBr3 perovskite films for efficient light-emitting diodes and amplified spontaneous emission. *Nat. Commun.* 16, 2367 (2025).
- Qin, F. et al. Highly efficient and flexible perovskite nanocrystal lightemitting diodes on disposable paper substrates. ACS Appl. Mater. Interfaces 15, 47278–47285 (2023).
- Zhao, J. et al. High-speed fabrication of all-inkjet-printed organometallic halide perovskite light-emitting diodes on elastic substrates. Adv. Mater. 33, 2102095 (2021).
- Zhang, Q. et al. Organic-inorganic hybrid perovskite quantum dot light-emitting diodes using a graphene electrode and modified PEDOT:PSS. RSC Adv. 9, 20931–20940 (2019).
- 58. Lu, M. et al. Highly flexible CsPbl3 perovskite nanocrystal light-emitting diodes. *ChemNanoMat* **5**, 313–317 (2019).
- Li, Y.-F. et al. Stretchable organometal-halide-perovskite quantumdot light-emitting diodes. *Adv. Mater.* 31, 1807516 (2019).
- Zhao, F. et al. Highly flexible organometal halide perovskite quantum dot based light-emitting diodes on a silver nanowire–polymer composite electrode. J. Mater. Chem. C. 5, 531–538 (2017).
- Cao, F. et al. Mixed-dimensional mxene-based composite electrodes enable mechanically stable and efficient flexible perovskite light-emitting diodes. *Nano Lett.* 22, 4246–4252 (2022).
- 62. Seo, H.-K. et al. Efficient flexible organic/inorganic hybrid perovskite light-emitting diodes based on graphene anode. *Adv. Mater.* **29**, 1605587 (2017).
- Park, J. K., Kim, S. Y., Kim, J. H., Heo, J. H. & Im, S. H. Spray-coated nanocrystalline CsPbBr3 perovskite thin-films for large area and efficient rigid and flexible light emitting diodes. *J. Alloy. Compd.* 918, 165560 (2022).
- 64. Hamanaka, V. N., Salsberg, E., Fonseca, F. J. & Aziz, H. Investigating the influence of the solution-processing method on the morphological properties of organic semiconductor films and their impact on OLED performance and lifetime. *Org. Electron.* **78**, 105509 (2020).
- Chu, S. et al. Large-area and efficient perovskite light-emitting diodes via low-temperature blade-coating. *Nat. Commun.* 12, 147 (2021).
- 66. Jin, F. et al. Morphology control towards bright and stable inorganic halide perovskite light-emitting diodes. *J. Mater. Chem. C.* **6**, 1573–1578 (2018).
- Jung, D. H. et al. Flash-induced ultrafast recrystallization of perovskite for flexible light-emitting diodes. *Nano Energy* 61, 236–244 (2019).

- Liu, H. et al. Large-area flexible perovskite light-emitting diodes enabled by inkjet printing. Adv. Mater. 36, 2309921 (2024).
- Chen, C. et al. Efficient flexible inorganic perovskite light-emitting diodes fabricated with CsPbBr₃ emitters prepared via lowtemperature in situ dynamic thermal crystallization. *Nano Lett.* 20, 4673–4680 (2020).
- Lu, J. et al. Dendritic CsSnl3 for efficient and flexible near-infrared perovskite light-emitting diodes. Adv. Mater. 33, 2104414 (2021).
- Zhou, C. et al. Low dimensional metal halide perovskites and hybrids. *Mater. Sci. Eng.: R Rep.* 137, 38–65 (2019).
- Zhu, L., Liu, D., Wang, J. & Wang, N. Large organic cations in quasi-2D perovskites for high-performance light-emitting diodes. *J. Phys. Chem. Lett.* 11, 8502–8510 (2020).
- Gupta, Y., Rathore, S., Singh, A. & Kumar, A. Tailoring the mechanical response of Ruddlesden Popper lead halide perovskites. J. Alloy. Compd. 901, 163575 (2022).
- Rathore, S., Leong, W. L. & Singh, A. Mechanical properties estimation of 2D–3D mixed organic-inorganic perovskites based on methylammonium and phenylethyl-ammonium system using a combined experimental and first-principles approach. *J. Alloy.* Compd. 936, 168328 (2023).
- Tu, Q. et al. Stretching and breaking of ultrathin 2D hybrid organic–inorganic perovskites. ACS Nano 12, 10347–10354 (2018).
- Zhang, L. et al. High-performance quasi-2D perovskite light-emitting diodes: from materials to devices. Light Sci. Appl. 10, 61 (2021).
- Zhao, L. et al. Influence of bulky organo-ammonium halide additive choice on the flexibility and efficiency of perovskite light-emitting devices. Adv. Funct. Mater. 28, 1802060 (2018).
- 78. Sun, C. et al. High-performance large-area quasi-2D perovskite light-emitting diodes. *Nat. Commun.* **12**, 2207 (2021).
- Wang, J. et al. Inkjet-printed full-color matrix quasi-two-dimensional perovskite light-emitting diodes. ACS Appl. Mater. interfaces 13, 41773–41781 (2021).
- Chirvony, V. S. et al. Achieving inkjet-printed 2D tin iodide perovskites: excitonic and electro-optical properties. *Adv. Funct. Mater.* 34, 2405154 (2024).
- Vescio, G. et al. 2D PEA2Snl4 inkjet-printed halide perovskite LEDs on rigid and flexible substrates. ACS Energy Lett. 7, 3653–3655 (2022).
- Bi, W. et al. Efficient quasi-two-dimensional perovskite lightemitting diodes with improved multiple quantum well structure. ACS Appl. Mater. Interfaces 12, 1721–1727 (2020).
- 83. Sun, Y. et al. The formation of perovskite multiple quantum well structures for high performance light-emitting diodes. *npj Flex. Electron.* **2**, 12 (2018).
- Rui, H. et al. Tunable deep-red electroluminescence from flexible quasi-2D perovskites light-emitting diodes. *IEEE Electron Device Lett.* 40, 59–62 (2019).
- Cheng, L. P. et al. Efficient CsPbBr3 perovskite light-emitting diodes enabled by synergetic morphology control. Adv. Opt. Mater. 7, 1801534 (2019).
- Zhang, D. et al. Metal halide perovskite nanowires: synthesis, integration, properties, and applications in optoelectronics. Adv. Energy Mater. 13, 2201735 (2023).
- 87. Aftab, S. et al. Lighting the future: perovskite nanorods and their advances across applications. *Nano Energy* **124**, 109504 (2024).
- 88. Lin, C.-H. et al. Giant optical anisotropy of perovskite nanowire array films. *Adv. Funct. Mater.* **30**, 1909275 (2020).
- Gu, L. et al. A biomimetic eye with a hemispherical perovskite nanowire array retina. *Nature* 581, 278–282 (2020).
- Ma, S. et al. Ultra-sensitive and stable multiplexed biosensors array in fully printed and integrated platforms for reliable perspiration analysis. Adv. Mater. 36, 2311106 (2024).
- Yuan, Z. et al. One-dimensional organic lead halide perovskites with efficient bluish white-light emission. Nat. Commun. 8, 14051 (2017).

- Jang, J. H., Li, S., Kim, D.-H., Yang, J. & Choi, M. K. Materials, device structures, and applications of flexible perovskite light-emitting diodes. Adv. Electron. Mater. 9, 2201271 (2023).
- Bi, C. et al. Self-assembled perovskite nanowire clusters for high luminance red light-emitting diodes. *Adv. Funct. Mater.* 30, 2005990 (2020).
- Zhang, Q. et al. Three-dimensional perovskite nanophotonic wire array-based light-emitting diodes with significantly improved efficiency and stability. ACS Nano 14, 1577–1585 (2020).
- Zhang, D. et al. Large-scale planar and spherical light-emitting diodes based on arrays of perovskite quantum wires. *Nat. Photonics* 16, 284–290 (2022).
- Cao, Y. B. et al. High-efficiency, flexible and large-area red/green/ blue all-inorganic metal halide perovskite quantum wires-based light-emitting diodes. *Nat. Commun.* 14, 4611 (2023).
- 97. Lê, K. et al. Electrospun Electroluminescent CsPbBr3 Fibers as Flexible Perovskite Networks for Light-Emitting Application. *Adv. Eng. Mater.* **25**, 2201651 (2023).
- Ren, B. et al. Full-color fiber light-emitting diodes based on perovskite quantum wires. Sci. Adv. 10, eadn1095 (2024).
- 99. Wei, R. et al. Revolutionizing wearable technology: advanced fabrication techniques for body-conformable electronics. *npj Flex. Electron.* **8**, 83 (2024).
- Huang, H., Bodnarchuk, M. I., Kershaw, S. V., Kovalenko, M. V. & Rogach, A. L. Lead Halide Perovskite Nanocrystals in the Research Spotlight: Stability and Defect Tolerance. ACS Energy Lett. 2, 2071–2083 (2017).
- Wang, Y.-K. et al. Long-range order enabled stability in quantum dot light-emitting diodes. *Nature* 629, 586–591 (2024).
- Chen, B. et al. Dual-Function self-assembled molecules as holetransport layers for thermally evaporated high-efficiency blue perovskite light-emitting diodes. Adv. Mater. 37, 2411451 (2025).
- Wang, H.-C., Bao, Z., Tsai, H.-Y., Tang, A.-C. & Liu, R.-S. Perovskite quantum dots and their application in light-emitting diodes. *Small* 14. 1702433 (2018).
- 104. Li, Y. et al. One-step preparation of long-term stable and flexible CsPbBr3 perovskite quantum dots/ethylene vinyl acetate copolymer composite films for white light-emitting diodes. ACS Appl. Mater. Interfaces 10, 15888–15894 (2018).
- Sun, C. et al. Highly luminescent, stable, transparent and flexible perovskite quantum dot gels towards light-emitting diodes. Nanotechnology 28, 365601 (2017).
- Bai, W. et al. Microscale perovskite quantum dot light-emitting diodes (Micro-PeLEDs) for full-color displays. *Adv. Opt. Mater.* 10, 2200087 (2022).
- Ali, M. A. et al. Modeling of structural, elastic, mechanical, acoustical, electronic and thermodynamic properties of XPdF3 (X= Rb, Tl) perovskites through density functional theory. *Phys. Scr.* 95, 075705 (2020).
- 108. Dai, Z. et al. The mechanical behavior of metal-halide perovskites: elasticity, plasticity, fracture, and creep. Scr. Mater. **223**, 115064 (2023).
- Li, K. et al. Electronic structures and elastic properties of a family of metal-free perovskites. *Mater. Chem. Front.* 3, 1678–1685 (2019).
- Kim, D., Vasileiadou, E. S., Spanopoulos, I., Kanatzidis, M. G. & Tu, Q. In-plane mechanical properties of two-dimensional hybrid organic-inorganic perovskite nanosheets: structure-property relationships. ACS Appl. Mater. Interfaces 13, 31642–31649 (2021).
- Zhang, Y. et al. Homogeneous freestanding luminescent perovskite organogel with superior water stability. *Adv. Mater.* 31, 1902928 (2019).
- Lei, Y. et al. Microstress for metal halide perovskite solar cells: from source to influence and management. *Nanoscale* 16, 2765–2788 (2024).
- Liu, D. et al. Strain analysis and engineering in halide perovskite photovoltaics. *Nat. Mater.* 20, 1337–1346 (2021).

- Baumann, S. et al. Stability and reliability of perovskite containing solar cells and modules: degradation mechanisms and mitigation strategies. *Energy Environ. Sci.* 17, 7566–7599 (2024).
- Boyd, C. C., Cheacharoen, R., Leijtens, T. & McGehee, M. D. Understanding degradation mechanisms and improving stability of perovskite photovoltaics. *Chem. Rev.* 119, 3418–3451 (2018).
- Jia, S. et al. Highly luminescent and stable green quasi-2D perovskite-embedded polymer sheets by inkjet printing. Adv. Funct. Mater. 30, 1910817 (2020).
- Li, T. et al. Polymer cross-linking strategy enables high performance and high mechanical stability flexible quasi-2D perovskite lightemitting diodes. Adv. Opt. Mater. 12, 2302053 (2024).
- Sung, C.-H. et al. Highly luminescent perovskite quantum dots for light-emitting devices: photopatternable perovskite quantum dot-polymer nanocomposites. J. Mater. Chem. C. 10, 15941–15947 (2022).
- Zang, J. et al. Self-healing perovskite films enabled by fluorinated cross-linked network targeting flexible light-emitting diode. Adv. Opt. Mater. 10, 2200566 (2022).
- Bade, S. G. R. et al. Stretchable light-emitting diodes with organometal-halide-perovskite-polymer composite emitters. *Adv. Mater.* 29, 1607053 (2017).
- 121. Sun, S. et al. Enhanced flexibility and stability of emissive layer enable high-performance flexible light-emitting diodes by cross-linking of biomass material. *Adv. Funct. Mater.* **32**, 2204286 (2022).
- Qian, X. et al. Bio-inspired pangolin design for self-healable flexible perovskite light-emitting diodes. ACS Nano 16, 17973–17981 (2022).
- 123. Zhao, X. & Tan, Z.-K. Large-area near-infrared perovskite light-emitting diodes. *Nat. Photonics* **14**, 215–218 (2020).
- Chou, S.-Y. et al. Transparent perovskite light-emitting touchresponsive device. ACS Nano 11, 11368–11375 (2017).
- Kwon, J. I. et al. Ultrahigh-resolution full-color perovskite nanocrystal patterning for ultrathin skin-attachable displays. Sci. Adv. 8. eadd0697 (2022).
- Shan, Q. et al. Perovskite light-emitting/detecting bifunctional fibres for wearable LiFi communication. Light Sci. Appl. 9, 163 (2020).
- Qin, F. et al. Paper substrates based flexible red-emitting perovskite nanocrystal light-emitting diodes. *IEEE Electron Device Lett.* 44, 1056–1059 (2023).
- Liu, Y. et al. Boosting the efficiency of quasi-2D perovskites lightemitting diodes by using encapsulation growth method. *Nano Energy* 80, 105511 (2021).

Acknowledgements

This work is supported by the National Key Research and Development Program of China (2024YFE0204600), Guangdong Key Laboratory of

Optoelectronic Materials and Chips under Grant No.2022KSYS014, Shenzhen Key Laboratory Project under Grant No.ZDSYS201603311644527, Longgang Key Laboratory Project under Grant No.ZSYS2017003 and No.LGKCZSYS2018000015. Q.Z. and X.M. thank the support of the State Key Laboratory of Photovoltaic Science and Technology (202401030303). Y.F. thanks the support of Fundamental Research Funds for the Central Universities, Sun Yat-sen University (76280-31610003).

Author contributions

Original draft writing: Y.L., T.G., Z.H., C.S., S.Z., and M.L. Manuscript modification: Y.L., T.G., Z.H., Z.Z., W.B., X.M., Y.F., Q.Z., D.Z. and Z.F. D.Z., Q.Z., Y.F., and Z.F. led the preparation of the manuscript. Y.L., T.G., and Z.H. contributed equally to the work.

Competing interests

The authors declare no competing interests.

Additional information

Correspondence and requests for materials should be addressed to Daquan Zhang, Qianpeng Zhang, Yu Fu or Zhiyong Fan.

Reprints and permissions information is available at http://www.nature.com/reprints

Publisher's note Springer Nature remains neutral with regard to jurisdictional claims in published maps and institutional affiliations.

Open Access This article is licensed under a Creative Commons Attribution-NonCommercial-NoDerivatives 4.0 International License, which permits any non-commercial use, sharing, distribution and reproduction in any medium or format, as long as you give appropriate credit to the original author(s) and the source, provide a link to the Creative Commons licence, and indicate if you modified the licensed material. You do not have permission under this licence to share adapted material derived from this article or parts of it. The images or other third party material in this article are included in the article's Creative Commons licence, unless indicated otherwise in a credit line to the material. If material is not included in the article's Creative Commons licence and your intended use is not permitted by statutory regulation or exceeds the permitted use, you will need to obtain permission directly from the copyright holder. To view a copy of this licence, visit https://creativecommons.org/licenses/by-nc-nd/4.0/.

© The Author(s) 2025